



Communication

Molecular hexagram and octagram: Position determined 3D metallo-supramolecules and concentration-induced transformation

Tun Wu^{a,1}, Zhiyuan Jiang^{b,1}, Xiaobo Xue^b, Shi-Cheng Wang^c, Mingzhao Chen^a, Jun Wang^b, Haisheng Liu^b, Jun Yan^b, Yi-Tsu Chan^c, Pingshan Wang^{a,b,*}^a Institute of Environmental Research at Greater Bay Area, Key Laboratory for Water Quality and Conservation of the Pearl River Delta, Ministry of Education, Guangzhou University, Guangzhou 510006, China^b Department of Organic and Polymer Chemistry, College of Chemistry and Chemical Engineering, Central South University, Changsha 410083, China^c Department of Chemistry, National Taiwan University, Taipei 10617

ARTICLE INFO

Article history:

Received 24 July 2020

Received in revised form 23 January 2021

Accepted 31 January 2021

Available online 3 February 2021

Keywords:

Self-assembly

Terpyridine

Supramolecular transformation

Metal-organic ligand

Metalla-cage

ABSTRACT

The reaction of a metallo-organic ligand (**LA**) in which two “V”-shaped bisterpyridines attaching to meta-position of “X”-shaped tetraterpyridine via <tpy-Ru²⁺-tpy > connectivity and Zn²⁺ ions gave rise to 3D supramolecular architectures: octagram (Zn₈**LA**₄). However, a position varied ligand (**LB**) in which two “V”-shaped bisterpyridines locating at the ortho-position of “X”-shaped tetraterpyridine afforded a different 3D hexagram (Zn₆**LB**₃). Full characterizations included NMR (¹H, ¹³C, 2D COSY, NOESY and DOSY), ESI-MS, TWIM-MS, TEM and AFM. The resulted structures were directly determined by the position of two “V”-shaped bisterpyridines attaching to “X”-shaped tetraterpyridine.

© 2021 Chinese Chemical Society and Institute of Materia Medica, Chinese Academy of Medical Sciences.

Published by Elsevier B.V. All rights reserved.

Coordination-driven self-assembly has developed to be an extremely effective approach toward 2D and 3D supramolecules with preprogrammed shapes, sizes and functions [1–8]. Among them, 3D metallo-supramolecular cages received continuing interests due to its fascinating structures and potential applications in the fields of host-guest chemistry [9,10], catalysis [11,12] and others [13–15]. 2,2':6',2''-Terpyridine (tpy) ligands are ideal subunits because of their tunable binding ability with various transition metal ions [16,17]. Newkome and others reported numerous 2D metallo-supramolecular architectures [18–21] by utilizing <tpy-M²⁺-tpy > connectivity (M = Zn, Cd, Ru, Fe, Os, Ir). Even so, construction of tpy-based 3D metallo-cages still remains great challenge, except for numbered successful examples [22–25]. Considering the self-assembly methodology, multitopic tpy ligands with noncoplanar binding sites are necessary to form the desired 3D cages due to the linear coordination geometry of <tpy-M²⁺-tpy > connectivity. Generally, these noncoplanar binding sites are connected by rigid or flexible linkages such as adamantane [22], crown ethers [24,25], and 9,10-dimethyl-9,10-ethanoanthracene

[23]. However, this ligand design strategy exhibits limitations because of synthetic difficulties and a limited number of organic scaffolds. Therefore, it is imperative to develop other effective approaches toward 3D metallo-cages. In addition, thermodynamic stability of the resulting 3D metallo-structures relies on multi-parameters including solvent [26], concentration [23,24], anion [27], light [28] and others [29]. Deep research of other influenced factors (position, geometry) provides profound understanding of the self-assembly process and further promotes this field.

Initially, our previous work demonstrated that simply mixing the “V”-shaped bis-terpyridine, tetrakis-terpyridine and Zn²⁺ with a precise 2:1:4 molar ratio afforded only self-sorted metallo-triangle [Zn₃V₃] [21]. Therefore, the pre-connection of two ligands using irreversible Ru coordination is necessary for quantitative assembly. A novel metallo-organic ligand **LA** has been prepared by linking two “V”-shaped bis-terpyridines to one “X”-shaped tetrakis-terpyridine's meta-positions via <tpy-Ru²⁺-tpy > connectivity. The angle between the uncomplexed tpy's of “V”-shaped ligands and the plane of “X”-shaped ligand is about 60° when **LA** adopts an energy-minimized conformation. Based on the directional binding approach, directly mixing **LA** and Zn²⁺ in a 1:2 molar ratio gave rise to 3D metallo-supramolecules: octagram **C**. Thus, 3D metal-organic cages can be achieved by using metal-organic ligands (MOLs) from the permutation of simple tpy ligands with appropriate geometry design. The rotatable coordination sites of

* Corresponding author at: Institute of Environmental Research at Greater Bay Area, Key Laboratory for Water Quality and Conservation of the Pearl River Delta, Ministry of Education, Guangzhou University, Guangzhou 510006, China.

E-mail address: chemwps@csu.edu.cn (P. Wang).

¹ These authors are contributed equally to this work.

LA in the self-assembly process led to the formation of flexible 3D supramolecular architectures (Scheme 1).

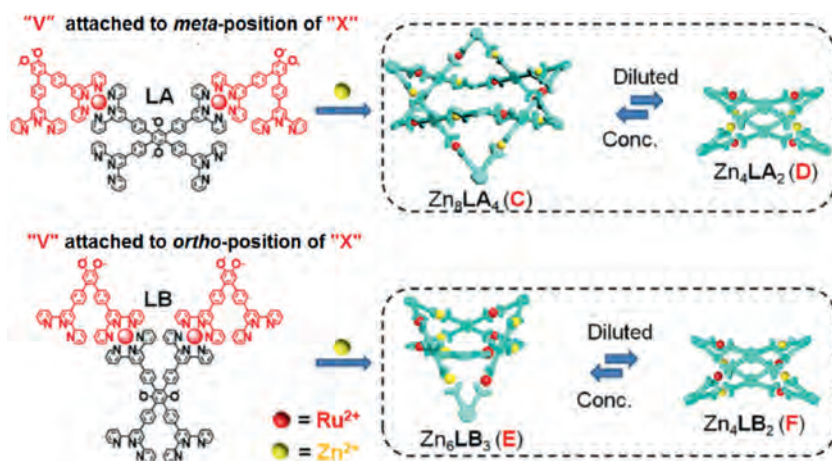
Tetratopic **LA** was synthesized in 5 steps starting from commercially available 2,6-dibromobenzene-1,4-diol (Scheme S1 in Supporting information). Then, to an MeCN solution of **LA**, a MeOH solution containing $\text{Zn}(\text{NO}_3)_2 \cdot 4\text{H}_2\text{O}$ was added in a precise 1:2 molar ratio.

After the mixture was stirred at 80 °C for 4 h, a saturated solution of NH_4PF_6 in MeOH was added to generate red precipitates, which were washed thoroughly with MeOH and H_2O . After drying *in vacuo* at 50 °C for 18 h, the desired octagram **C** was obtained in 98% yield with PF_6^- counterions. The ESI-MS spectrum of octagram **C** (4 mg/mL in MeCN) showed one set of dominant peaks resulting from the ions with the charge states from 18+ to 9+ generated by losing the corresponding numbers of PF_6^- . The experimental isotope patterns for each charge state agreed well with the corresponding theoretical distributions (Fig. 1c and Fig. S35 in Supporting information). The 2D TWIM-MS plot of octagram **C** showed a single distribution with narrow drift times for the charge states ranging from 19+ to 13+, indicating formation of a single component. However, a charge-dependent conformation transition at 12+ charge state was observed, suggesting that 3D octagram **C** has certain structural flexibility (Fig. S40 in Supporting information) [21]. The experimental average collision cross-section (CCS) of $1868.4 \pm 154.1 \text{ \AA}^2$ for all charge states derived from the TWIM-MS analysis was in good agreement with the theoretical value of $1863.5 \pm 98.8 \text{ \AA}^2$ generated by trajectory method (TM) in MOBICAL based on 200 annealed structures (Table S1 in Supporting information) [30]. The relatively large standard deviation also reflected its conformational flexibility. The structure of **C** was verified by ^1H NMR spectroscopy as well (Fig. 1b), which showed four singlets at δ 9.06, 9.03, 9.02 and 8.99 with a 1:1:1:1 integration ratio assigned to 3',5' protons of tpy-A, B, C, D respectively. The peaks for 6,6'' protons of the uncoordinated tpy's in **LA** (tpy-C, D) exhibited a dramatic upfield shift from 8.72 ppm to 7.84 ppm (Figs. 1a and b, $\Delta\delta = -0.88$) owing to the electron shielding effect [31]. In the non-aromatic region, a broad singlet at δ 4.03 and two sharp singlets at δ 3.26 and δ 3.25 in a 4:1:1 integration ratio attributed to the methoxy groups close to tpy-C, D, tpy-A and tpy-B, respectively. In theory, self-assembly from **LA** and Zn^{2+} can afford two structures: octagram **C** and possible **G** (Fig. S48 in Supporting information). The composition (Zn_8LA_4) of the possible isomer **G** is the same as octagram **C** which cannot be distinguished by mass spectroscopy. However, in principle, NMR spectroscopy can rule out other isomers. Compared to highly symmetric octagram **C** (the chemical environmental of

four **LA**s is identical), the possible isomer **G** is less symmetrical which suggesting two kinds of chemical environment of **LA**. ^1H NMR of possible **G** will exhibit eight kinds of signals for tpy units. As a matter of fact, ^1H NMR result revealed four kinds of tpy signals which fully validated the generation of octagram **C**. All proton assignments for octagram **C** were further confirmed by 2D COSY and NOESY NMR (Figs. S22 and S23 in Supporting information). The diffusion-ordered spectroscopy (DOSY) NMR spectrum of **C** in CD_3CN at 25 °C showed a narrow band, clearly demonstrating there was only a single component in solution (diffusion coefficient $\log D = -9.81 \text{ m}^2/\text{s}$, Fig. S24 in Supporting information) [32]. The above evidences have proved the formation of octagram **C**.

Subsequently, an interesting concentration-triggered supramolecular transformation process was observed by ESI-MS. A portion of octagram **C** was dissociated into smaller supramolecular species after diluting with MeCN (0.1 mg/mL). As we can see from the ESI-MS spectrum, the isotope patterns of the even charge states (20+, 18+, and 16+) exhibited two kinds of supramolecular species, which were consistent with the corresponding theoretical distributions of octagram **C** and another new structure (Fig. S32 in Supporting information). Further decreasing the concentration to 10 $\mu\text{g}/\text{mL}$, the original ESI-MS signals of octagram **C** disappeared completely, whereas only a new series of intense peaks corresponding to the 10+ to 5+ ions were observed, which confirmed the formation of a different structure with an exactly half molecular weight of octagram **C** (Fig. 1d). The newly generated species consisting of two **LA** and four Zn^{2+} ions suggested the formation of 3D tetragonal bipyramid **D**. In addition, the TWIM-MS plot of **D** exhibited a series of narrow drift times, which revealed the absence of other isomers or conformers (Fig. S41 in Supporting information). The proposed structure was further corroborated by the experimental average CCS ($963.3 \pm 22.2 \text{ \AA}^2$) deduced from its TWIM-MS drift time that was consistent with the simulated TM value ($1005.1 \pm 22.9 \text{ \AA}^2$, Table S2 in Supporting information).

Further, slight variation of metal-organic ligand in which two "V"-shaped bis-terpyridines binding to the *ortho*-position of "X"-shaped tetrakis-terpyridine afforded a novel and similar ligand **LB**. After complexation with 2 equiv. Zn^{2+} ions, ^1H NMR spectra of the product **E** showed broad resonances which indicative of a giant structure (Figs. 2a and b) [33,34]. Signals assigned to 6,6''-tpy protons of free tpy units were distinctly shifted upfield from 8.65 ppm to 7.84 ppm ($\Delta\delta = 0.81 \text{ ppm}$). In 2D DOSY NMR spectrum, the formation of a single assembly in CD_3CN was evident from the diffusion coefficient of $\log D = -9.76 \text{ m}^2/\text{s}$ for all the relevant peaks (Fig. S28 in Supporting information). Further, ESI-MS has been performed to establish the composition of the generated structure



Scheme 1. Self-assembly of 3D octagram **C**, tetragonal bipyramid **D**, hexagram **E**, and tetragonal bipyramid **F**.

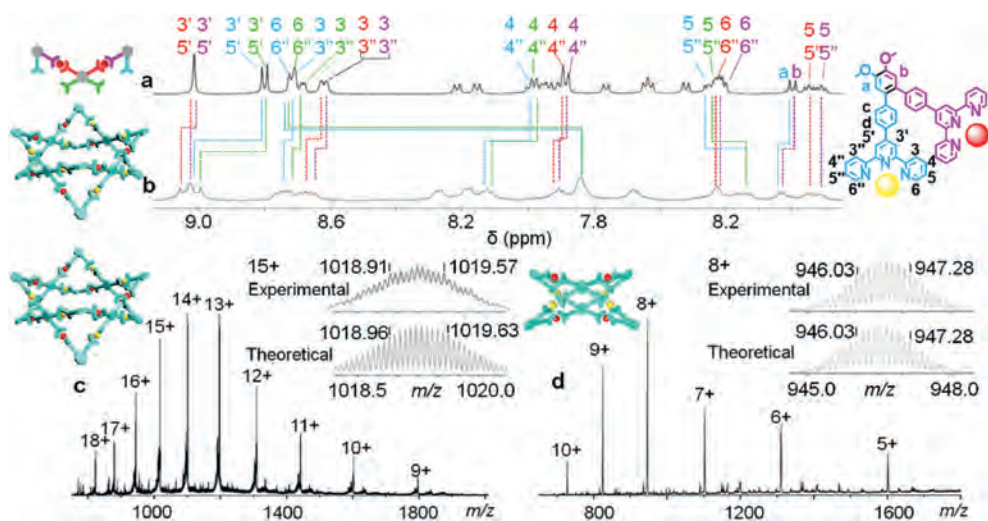


Fig. 1. ¹H NMR spectra (500 MHz, CD₃CN, 25 °C) of (a) LA and (b) octagram C, ESI-MS spectra (in MeCN) of (c) C (4 mg/mL) and (d) tetragonal bipyramid D (10 μg/mL).

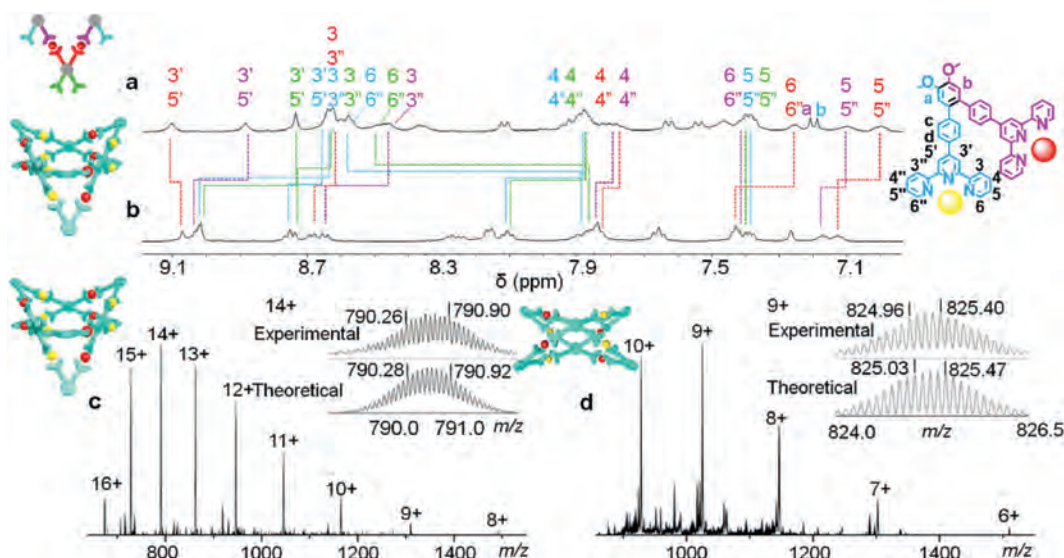


Fig. 2. ¹H NMR spectra (500 MHz, CD₃CN, 25 °C) of (a) LB and (b) hexagram E, ESI-MS spectra (in MeCN) of (c) E (4 mg/mL) and (d) tetragonal bipyramid F (10 μg/mL).

[Zn₆LB₃] (4 mg/mL) which displaying nine prominent peaks with expected isotopic patterns corresponding to charge state from 16 + to 8+ (Fig. 2c). In 2D TWIM-MS plot, all the charge states were found at a narrow band, suggesting a single component with high conformational rigidity. Slight variation between LA and LB caused two entirely different structures: octagram C and hexagram E, reflecting the position factor which is of easy ignoring profoundly influenced the self-assembly process. Likewise, diluting the solution of hexagram E in MeCN gave rise to a new structure: tetragonal bipyramid F (10 μg/mL). ESI-MS revealed a new set of dominant peaks ranging from 10+ to 6+ ions with explicit isotope patterns (Fig. 2d). It is worth noting the reversible concentration-dependent transformation is believed to be driven by entropic forces [35,36].

Finally, atomic force microscopy (AFM) was utilized to visualize the individual resultant supermolecules. The AFM image of a mixture of C and D (4.0 ± 0.2 nm and 2.0 ± 0.2 nm), which were very close to the simulated heights of octagram C (4.1 nm) and tetragonal bipyramid D (1.9 nm) (Fig. 3) at a concentration of 5 × 10⁻⁶ mol/L on mica displayed scattered small dots with two different heights (4.2 ± 0.3 nm).

In conclusion, two novel 3D tpy-based octagram and hexagram have been successfully prepared from two pre-designed metal-organic ligands. The great differences of the resulting structure caused by slight variation of geometric location for two “V”-shaped bisterpyridines (from tetraterpyridine’s *meta*-position to *ortho*-

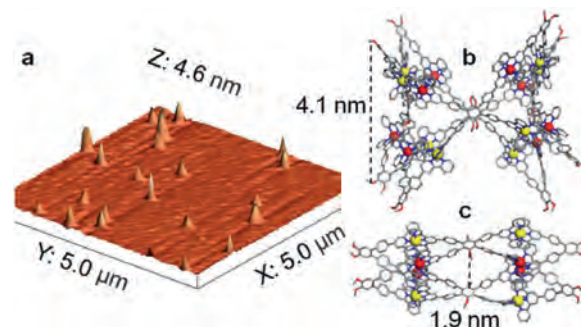


Fig. 3. (a) AFM image of a mixture of C and D, representative energy-minimized structures of (b) C, (c) D.

position). Further, upon dilution, these two metallo-cages can split into smaller tetragonal bipyramid structures (**E**, **F**) (Scheme 1). MOLs prepared by a stepwise strategy offer rapid access to construction of 3D tpy-based supramolecular structures, and the unique supramolecular transformation process will be beneficial to develop stimuli-responsive functional materials.

Declaration of competing interest

The authors declare that they have no known competing financial interests or personal relationships that could have appeared to influence the work reported in this paper.

Acknowledgments

This research was supported by the National Natural Science Foundation of China (No. 21971257 for P. Wang); Y.-T. Chan acknowledges the support from the Ministry of Science and Technology of Taiwan (No. MOST106-2628-M-002-007-MY3). Authors acknowledge the NMR and TEM measurements from The Modern Analysis and Testing Center of Central South University of China.

Appendix A. Supplementary data

Supplementary material related to this article can be found, in the online version, at doi:<https://doi.org/10.1016/j.ccl.2021.01.052>.

References

- [1] Y. Sun, C. Chen, J. Liu, et al., *Chem. Soc. Rev.* 49 (2020) 3889–3919.
- [2] T. Sawada, Y. Inomata, K. Shimokawa, et al., *Nat. Commun.* 10 (2019) 5687–6595.
- [3] G.Y. Wu, X. Shi, H. Phan, et al., *Nat. Commun.* 11 (2020) 3178–3188.
- [4] G.R. Newkome, C.N. Moorefield, *Chem. Soc. Rev.* 44 (2015) 3954–3967.
- [5] S.J. Dalgarno, N.P. Power, J.L. Atwood, *Coord. Chem. Rev.* 252 (2008) 825–841.
- [6] F. Wurthner, C.C. You, C.R. Saha-Möller, *Chem. Soc. Rev.* 33 (2004) 133–146.
- [7] J.R. Nitschke, *Acc. Chem. Res.* 40 (2007) 103–112.
- [8] S.J. Lee, W. Lin, *Acc. Chem. Res.* 41 (2008) 521–537.
- [9] R.J. Li, J.J. Holstein, W.G. Hiller, et al., *J. Am. Chem. Soc.* 141 (2019) 2097–2103.
- [10] B. Chen, J.J. Holstein, S. Horiuchi, *J. Am. Chem. Soc.* 141 (2019) 2097–2103.
- [11] S.M.M. Mulders, J.S. Zarra, J.R. Nitschke, *J. Am. Chem. Soc.* 135 (2013) 7039–7046.
- [12] J.S. Mugridge, A. Zahl, R.V. Eldik, et al., *J. Am. Chem. Soc.* 135 (2013) 4299–4306.
- [13] M. Yamashina, Y. Sei, M. Akita, et al., *Nat. Commun.* 5 (2014) 4662–4668.
- [14] M. du Plessis, V.I. Nikolayenko, L.J. Barbour, *J. Am. Chem. Soc.* 142 (2020) 4529–4533.
- [15] V. Croué, S. Goeb, G. Szalákyi, et al., *Angew. Chem. Int. Ed.* 55 (2016) 1746–1750.
- [16] D. Armspach, M. Cattalini, E.C. Constable, et al., *Chem. Commun.* 15 (1996) 1823–1824.
- [17] A. Wild, A. Winter, F. Schlütter, et al., *Chem. Soc. Rev.* 40 (2011) 1459–1511.
- [18] G.R. Newkome, P. Wang, C.N. Moorefield, et al., *Science* 312 (2006) 1782–1785.
- [19] Y. Li, Z. Jiang, M. Wang, et al., *J. Am. Chem. Soc.* 138 (2016) 10041–10046.
- [20] J.H. Fu, Y.H. Lee, Y.J. He, Y.T. Chan, *Angew. Chem. Int. Ed.* 54 (2015) 6231–6235.
- [21] T. Wu, Y.-S. Chen, M. Chen, et al., *Inorg. Chem.* 56 (2017) 4065–4071.
- [22] C. Wang, X.Q. Hao, M. Wang, et al., *Chem. Sci.* 5 (2014) 1221–1226.
- [23] T.Z. Xie, K. Guo, Z. Guo, et al., *Angew. Chem. Int. Ed.* 54 (2015) 9224–9229.
- [24] T.Z. Xie, K.J. Endres, Z. Guo, et al., *J. Am. Chem. Soc.* 138 (2016) 12344–12347.
- [25] Y.C. Wang, Y.P. Liang, J.Y. Cai, et al., *Chem. Commun.* 52 (2016) 12622–12625.
- [26] K. Suzuki, M. Kawano, M. Fujita, *Angew. Chem. Int. Ed.* 46 (2007) 2819–2822.
- [27] D. Preston, A. Fox-Charles, W.K.C. Lo, et al., *Chem. Commun.* 51 (2015) 9042–9045.
- [28] M. Han, R. Michel, B. He, et al., *Angew. Chem. Int. Ed.* 52 (2013) 1319–1323.
- [29] W. Wang, Y.X. Wang, H.B. Yang, *Chem. Soc. Rev.* 45 (2016) 2656–2693.
- [30] M.F. Mesleh, J.M. Hunter, A.A. Shvartsburg, et al., *J. Phys. Chem.* 100 (1996) 16082–16086.
- [31] N.M. Logacheva, V.E. Baulin, A.Y. Tsvadze, et al., *Dalton Trans.* 14 (2009) 2482–2489.
- [32] H. Lee, R.M. Venable, A.D. MacKerell Jr., *Biophys. J.* 95 (2008) 1590–1599.
- [33] Q.F. Sun, S. Sato, M. Fujita, *Nat. Chem.* 4 (2012) 330–333.
- [34] S.P. Black, A.R. Stefankiewicz, M.M.J. Smulders, et al., *Angew. Chem. Int. Ed.* 52 (2013) 5749–5752.
- [35] M. Fujita, O. Sasaki, T. Mitsuhashi, et al., *Chem. Commun.* 13 (1996) 1535–1536.
- [36] T. Kraus, M. Budesinsky, J. Cvacka, et al., *Angew. Chem. Int. Ed.* 45 (2006) 258–261.